Engineered Science

RESEARCH PAPER

View Article Online

Efficiency Enhancement for Cocktail Dye Sensitized Nb_2O_5 Photoanode Towards Dye Sensitized Solar Cell

Niyamat I. Beedri,[1] Prashant K. Baviskar,[1] Mahadeo Mahadik,[2] Sandesh R. Jadkar,[1] Jum Suk Jang[2] and Habib M. Pathan[1*]

In present report, we have developed Nb_2O_5 photoelectrode sensitized with cocktail dye as sensitizer towards enhancement in efficiency. The absorbance spectrum of pristine organic dyes viz. coumarin 343 (C343) and mercurochrome (MC) along with mixture of C343 and MC (cocktail) dye was recorded using UV-visible spectroscopy. The performances of Nb_2O_5 based photoanode were characterized using photocurrent density-voltage (J-V) measurement and the comparison of output photovoltaic performance for C343, MC and cocktail dye were discussed in detailed. Cocktail dye sensitization shows enhancement in short-circuit current density (J_{sc}) due to the complementary absorption of the two pristine sensitizers. The value of open circuit voltage (V_{oc}) for device sensitized using cocktail dye comes between the individual V_{oc} for pristine dye sensitized devices. Electrochemical impedance spectroscopy (EIS) was studied to understand the charge transfer. Based on EIS measurements, the increased efficiency value of the solar cell with the cocktail dye sensitized photoanode can be attributed to suppression of charge recombination at Nb_2O_5|dye|electrolyte interfaces and enhancement of electron transport in the photoanode along with the longer electron lifetime. The overall conversion efficiency reaches 0.70% for cocktail dye sensitized device.

Keywords: Nb_2O_5; Cocktail dye; Dye sensitized solar cell; Electrochemical characterization

Received 22 February 2019**, Accepted** 11 March 2019

DOI: 10.30919/es8d803

1. Introduction

The performance of dye sensitized solar cell (DSSCs) is mainly depend upon four component viz. (i) photoanode material, (ii) light absorbing material (dye), (iii) electrolyte and (iv) counter electrode.[1] Usually, nanocrystalline titanium dioxide (TiO_2) has been used as photoanode material in DSSCs; other than TiO_2 different metal oxide nanostructure such as zinc oxide (ZnO), tin oxide (SnO_2), zirconia (ZrO_2) and niobium pentaoxide (Nb_2O_5) were also used as photoanode material.[2-6] Nb_2O_5 as photoanode material has been attracting significant research interest due to it higher conduction band energy level than traditional TiO_2 and thus in principle produces higher open circuit voltage and comparable electron injection efficiency as well as better chemical stability.[7-9] The large surface area of the photoanode doesn't promise higher photocurrent and dye adsorption. The dye adsorption depends on the interaction of photoanode material with dye molecule.[10] The most efficient Nb_2O_5 photoanode based DSSCs reported so far was sensitized with Ru-complex dye.[11-15] Ru metal dyes were expensive to utilize while organic dye have some advantage like cost effective, eco-friendly, high molar extinction coefficient.[16] To the best of our knowledge and from literature survey; organic dye sensitized with Nb_2O_5 was only our earlier report with rose bengal for DSSCs application.[17] In contrast organic dyes like coumarin 343 (C343) and mercurochrome (MC) dye where emerged out to use as sensitizer with Nb_2O_5 photoanode based DSSCs. However; two diverse organic dyes having different absorption in visible region of solar spectrum were combined together to develop cocktail dye. This cocktail dye is responsible towards the enhancement of absorption spectrum in visible region. If absorption spectrum of dye increases then the light harvesting ability also increases. This corresponds to improvement in the performance of DSSCs.[18] Few reports are available on enhancement of photovoltaic parameter of DSSCs with combination of two dyes having complimentary absorption spectra. The comparison of efficiency with reported literature is summarized in table 1.[19-30] To best of our knowledge not a single attempt was made for C343, MC dyes along with cocktail dye as a sensitizer for Nb_2O_5 based photoanode towards DSSCs application.

In the present work, the attempt has been made to fabricate colorful and low cost DSSCs by using inexpensive dyes. The performance of C343, MC and cocktail dye sensitized Nb_2O_5 photoanode based DSSCs was tested and compared. The enhancement in performance of Nb_2O_5 based DSSCs sensitized with cocktail dye prepared by mixing C343 and MC dyes resulting to broadening of absorption spectra in visible region.

2. Experimental

2.1 Preparation of ZnO/Nb_2O_5 Photoanode

All chemicals and solvent were purchased from commercial chemical suppliers and used as received without further purification.

Prior to the deposition of porous Nb_2O_5; the modification of FTO was done by coating compact ZnO layer by successive ionic layer adsorption and reaction technique in similar way as reported earlier.[31] The Zinc acetate was used as the source of Zn^+ ion and ammonia were used as complexing agent. The aqueous ammonium zincate complex ion $\{[Zn(NH_3)_4]^{2+}\}$ was prepared by mixing 0.05 M $Zn(CH_3COO)_2$

[1]*Advanced Physics Laboratory, Department of Physics, Savitribai Phule Pune University, Pune-411007, India*

[2]*Division of Biotechnology, College of Environmental and Bioresource Sciences, Chonbuk National University, Iksan 570-752, Korea*

***E-mail:** pathan@physics.unipune.ac.in*

Table 1 Performance comparison of dye sensitized solar cells for individuals and cocktail dye sensitized various photoanodes.

Photoanode	Dyes	η	Ref
ZnO	D131	1.77	19
	D149	3.89	
	D149+ D131	4.1	
ZnO	EY	1.98	20
	MC	1.16	
	EY+MC	2.45	
TiO_2	SQ2	4.11	21
	JD1	5.44	
	JD1+SQ2	6.36	
TiO_2	D131	5.06	22
	Black dye	10.04	
	D131+black dye	11.0	
TiO_2	C106	9.5	23
	D131	5.6	
	C106+D131	11.1	
TiO_2	LD12	7.5	24
	CD5	5.7	
	LD12+CD5	9.0	
TiO_2	SQ1	4.23	25
	JK2	7.0	
	SQ1+JH-1	7.38	
TiO_2	SQ2	2.81	26
	JH-1	5.1	
	SQ2+JH-1	6.31	
TiO_2	D35	5.5	27
	DB	7.3	
	D35+ DB	8.7	
TiO_2	SPSQ2	3.95	28
	N3	7.13	
	SPSQ2+N3	8.20	
TiO_2	RED	3.36	29
	BLUE	1.56	
	RED+BLUE	4.00	
TiO_2	Zn-tri-PcNc1	2.38	30
	DH44	5.16	
	Zn-tri-PcNc1+ DH44	6.61	
Nb_2O_5	C343	0.35	**Present work**
	MC	0.64	
	C343+MC	0.70	

$2H_2O$ with NH_3 and the pH value of the resultant solution was maintained in between 11 and 12. ZnO compact layer was deposited on FTO coated glass substrate as first immersion of the substrate in ammonium zincate {$[Zn(NH_3)_4]^{2+}$} bath kept at 27 °C for complex adsorption for 5 s then immersion of the withdrawn substrates in hot water (90 °C) to form solid ZnO layer for 10 s this complete one deposition cycle like this we have carried out 25 cycle for preparation of ZnO compact layer after this ZnO compact film were annealed at 300 °C for 1hr. In the present work, Nb_2O_5 powder was synthesized by simple and low cost chemical method as reported.[17] Briefly, for the preparation of Nb_2O_5 powder niobium pentachloride ($NbCl_5$), hydrogen peroxide (H_2O_2) as oxidizing agent and acetic acid was used as a stabilizer was used.[32] Initially, 0.05 M solution of $NbCl_5$ in 100 ml DDW was prepared by constant stirring for 60 min at room temperature. Then prepare the mixture of acetic acid and H_2O_2 (1:5 volume ratio) in separate beaker. Add the mix solution drop wise in $NbCl_5$ solution with stirring at room temperature until homogeneous solution was formed. After this remove the solution from the beaker and centrifuge it for 20 min at 3000 rpm. Finally, the collected white powder was dried in incubator at 50 °C for 60 min followed by annealed at 700 °C for 1h to get pure orthorhombic phase. The Nb_2O_5 paste was prepared similarly as reported earlier[33] by using above synthesized Nb_2O_5 nanoparticle, ethyl cellulose, α-terpineol and ethanol. The prepared paste was deposited over compact ZnO layerby using doctor blade method. After 15 min of drying, films were annealed for 1 h at 450 °C.

2.2 Instrumentation

The photoanode was characterized by X-ray diffraction (Bruker D8 with Cu-kα, λ = 1.5406 Å) in the range of 20-80 degree. Raman spectra were recorded using a Jobin Yvon Horibra LAB RAM-HR spectrometer equipped with a He-Ne laser. The excitation wavelength is 532 nm and output power is 50 mW with resolution of the spectrometer is 1 cm^{-1}. Surface morphology and cross-section SEM was observed by using SEM technique (JOEL JSM 6360) and energy dispersive X-ray spectroscopy (EDS) is used to study the element constitution from the film. The optical absorption spectra of dyes ware recorded using UV-Vis spectrophotometer (JASCO V-670) in the range of 350-600nm.

2.3 Fabrication of DSSCs

The annealed ZnO/Nb_2O_5 photoanode were immersed for 24 h in 0.5 mM C343, MC and cocktail (C343:MC::1:1 volume ratio) dye solution prepared in ethanol dye at room temperature. The platinum coated FTO glass was used as counter electrode. The liquid electrolyte was prepared by dissolving 0.5 M tetra-n-propylammonium iodide and 0.1 M iodine in an ethylene carbonate and acetonitrile mixed solvent (20:80 by volume). Then the prepared polyiodide electrolyte was introduced between dye loaded photoanode which was then coupled with a Pt counter electrode using binder clips. The photovoltaic performance of the assembled devices has been studied using a Keithley source meter 2420 under illumination of light at 80 mW/cm^2 intensity with 0.25 cm^2 active area for all cells. The electrochemical impedance spectroscopy (EIS) measurements for DSSCs were carried out using potensiostat/galvanostat (IVIUM:Vertex) to study the Nb_2O_5/dye/electrolyte interface in the frequency domain of (10^6-10^0 Hz) under dark and applied voltage was open circuit voltage (0.7 V).

3. Results and Discussion

3.1 Structural Characterization

The X-rays diffraction pattern and Raman spectra for compact ZnO, bare Nb_2O_5 and ZnO/Nb_2O_5 photoanode are shown in Fig. 1 (a) and (b), respectively. The obtain XRD pattern (Fig. 1(a)) were compared with standard data and is found to be matches with the JCPDS card no. 27-1003 for Nb_2O_5 and JCPDS card no. 36-1451 for ZnO which confirm the formation of orthorhombic crystal structure of Nb_2O_5 and wurtzite Structure showing hexagonal phase for ZnO. High intense peak along (100), (002), (101) plane confirmed the growth of ZnO over FTO substrate. Whereas bare Nb_2O_5 film deposited on FTO substrate shows polycrystalline nature with orientations along (100), (180) and (181) planes. The XRD pattern of ZnO/Nb_2O_5 photoanode confirms the presence of ZnO as well as Nb_2O_5.

The Raman spectra for compact ZnO, bare Nb_2O_5 and ZnO/Nb_2O_5 photoanode are shown in Fig. 1 (b). The Raman band was assigned to the Raman active mode for the ZnO at 438 cm^{-1}.[34] For the bare Nb_2O_5 photoanode shows the strong broad peak at around 702 cm^{-1} dominates spectrum and other peak are also observed at around 232 and 126 cm^{-1} which further confirm that Nb_2O_5 is orthorhombic.[35-38] The Raman spectra of ZnO/Nb_2O_5 film shows the shift in Raman band and it is observe at 433 cm^{-1} corresponds to ZnO and 691 cm^{-1} strong broad peak and 237, 131 cm^{-1} weaker feature of Nb_2O_5 which confirm the results are in good agreement with the XRD measurements.

3.2 Morphological and element analysis

Fig. 2 (a) and (b) shows top view SEM image of compact ZnO layer and porous Nb_2O_5 photoanode over ZnO, respectively. ZnO/Nb_2O_5 image show highly dense and granular shape with porous morphology. Fig. 2(c) shows cross-sectional view of ZnO/Nb_2O_5 photoanode showing 16 μm thicknesses. The EDS pattern and cross-sectional

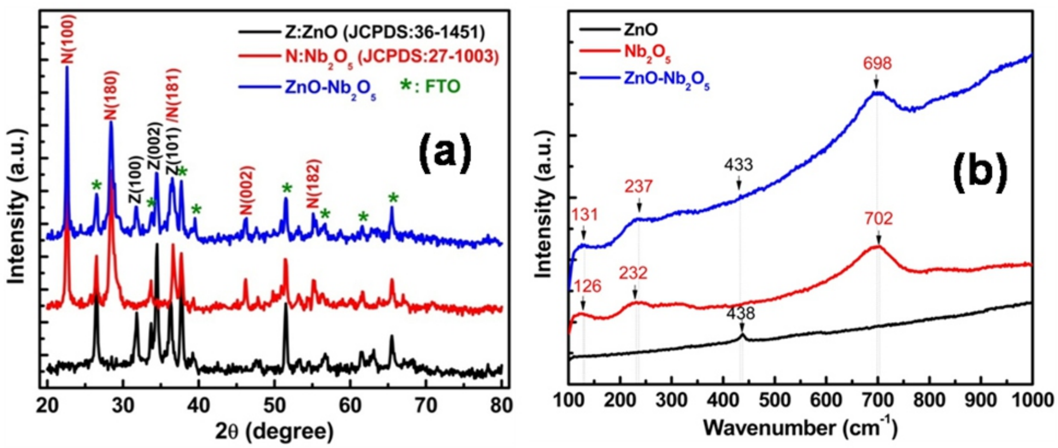

Fig. 1 (a) X-ray diffraction pattern and **(b)** Raman spectra of ZnO, Nb_2O_5 and ZnO/Nb_2O_5 films.

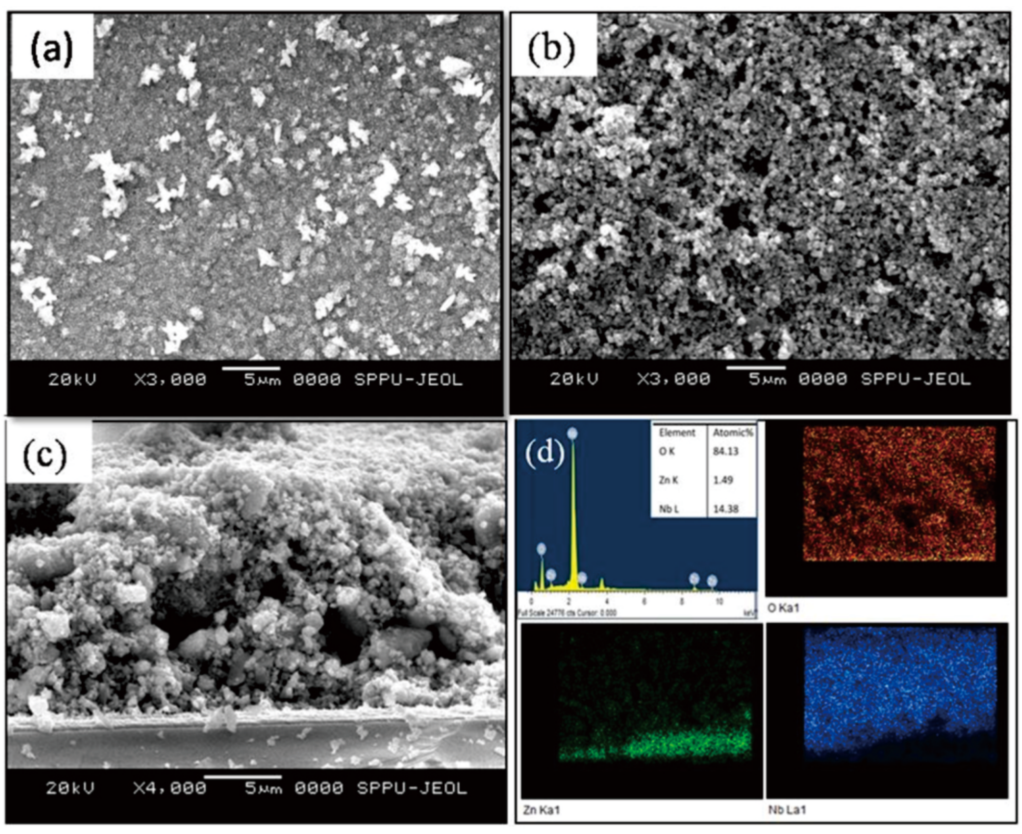

Fig. 2 (a) SEM image of compact ZnO,**(b)** porous Nb_2O_5 over ZnO film and **(c)** cross-section SEM of ZnO/Nb_2O_5. **(d)** Cross-sectional EDS spectra and mapping of ZnO/Nb_2O_5 film whereas inset show the elemental composition in atomic%.

mapping of ZnO/Nb_2O_5 photoanode is depict as Fig. 2(d); which confirms the presence of Nb, Zn and O in the film. The atomic % of all above elements from ZnO/Nb_2O_5 film was tabulated and shown as inset.

3.3 Optical absorption measurements

Fig. 3(a) shows the optical absorbance for ethanolic solutions of C343, MC and cocktail dye as a function of wavelength. Absorptions ranges were observed for C343 dye between 380-510 nm and for MC dye absorption region were seen from 450-545 nm, similarly for cocktail dye, two characteristics peaks were observed at 453 and 536 nm with increase in the visible absorption region from 365-585 nm. The increase in absorption region of dye was achieved by using cocktail dye prepared by mixing C343 and MC dyes. The Nb_2O_5 photoanode based DSSCs where fabricated by using C343, MC and cocktail dye. The enhancement in performance of Nb_2O_5 based DSSCs sensitized with cocktail dye prepared was observe due to increase in absorption spectra of cocktail dye in visible region Furthermore, the dye sensitized films were immersed in aqueous solution of 0.1 M NaOH to obtain the desorbed dye solutions. The amount of dye adsorbed over the Nb_2O_5 based films were calculated and summarised in table 1 by recording the absorbance spectra of desorbed dye solutions.

3.3 Characterization of DSSCs

3.3.1 J–V characterization

Fig. 3(b) shows the JV characteristics of DSSCs fabricated using Nb_2O_5 based photoanode sensitized with C343, MC and cocktail dye. The dye adsorption time was optimized as 24 h. The cell area of 0.25 cm^2 was used. The cell performance was observed under light (80 mW/cm^2). The photovoltaic parameter the solar cells such as open circuit voltage (V_{oc}), short circuit current density (J_{sc}), fill factor (FF) and efficiency (η) ware calculated and the values are summarised in table1. It is observed that the 50% & 9% enhancement in performance of Nb_2O_5 based DSSCs were observe for cocktail dye as compared to individual C343 & MC dye sensitized Nb_2O_5 based DSSCs, respectively.

3.3.2 EIS Analysis

The results of EIS analysis measured under dark were presented in Fig. 3(c & d). Fig. 3(c) shows the nyquist plots for C343, MC and cocktail dye sensitized devices. Usually, three semicircles in the nyquist plots were observed.[39] In the present case, only two semi-circles are observed: out of two the small semicircles in the high frequency region and large semicircles in the low frequency region corresponded to the charge transfer at the interface of counter electrode|electrolyte and electron recombination resistance at the interface Nb_2O_5|dye|electrolyte. It observed that the radius of semicircles in mid frequency region increases in the order of C343<MC<cocktail dye which is fascinating to note that there is considerably large electron recombination resistance (R_{ct}) resulting less electron recombination for device fabricated with cocktail dye compared to individual MC and C343 dye based device.[40] The enhancement in V_{oc} for cocktail dye sensitized device compared to C343 dye sensitized solar cell might be due to the steric effect[41] that can effectively prevent the transfer of I_3^- of the surface of Nb_2O_5. This could be responsible for the getting higher performance for cocktail dye sensitized device. The Bode phase plot shows the signature peak which represents interfacial electron recombination towards low frequency region for the cocktail dye compared to that of MC and C343 dye sensitized DSSCs (Fig. 3(d)). Electron life time were calculated from bode plot using formula $\tau_e = 1/2\pi f$.[42] The electron life time for the cell sensitized with cocktail dye was found to be larger compaired to the

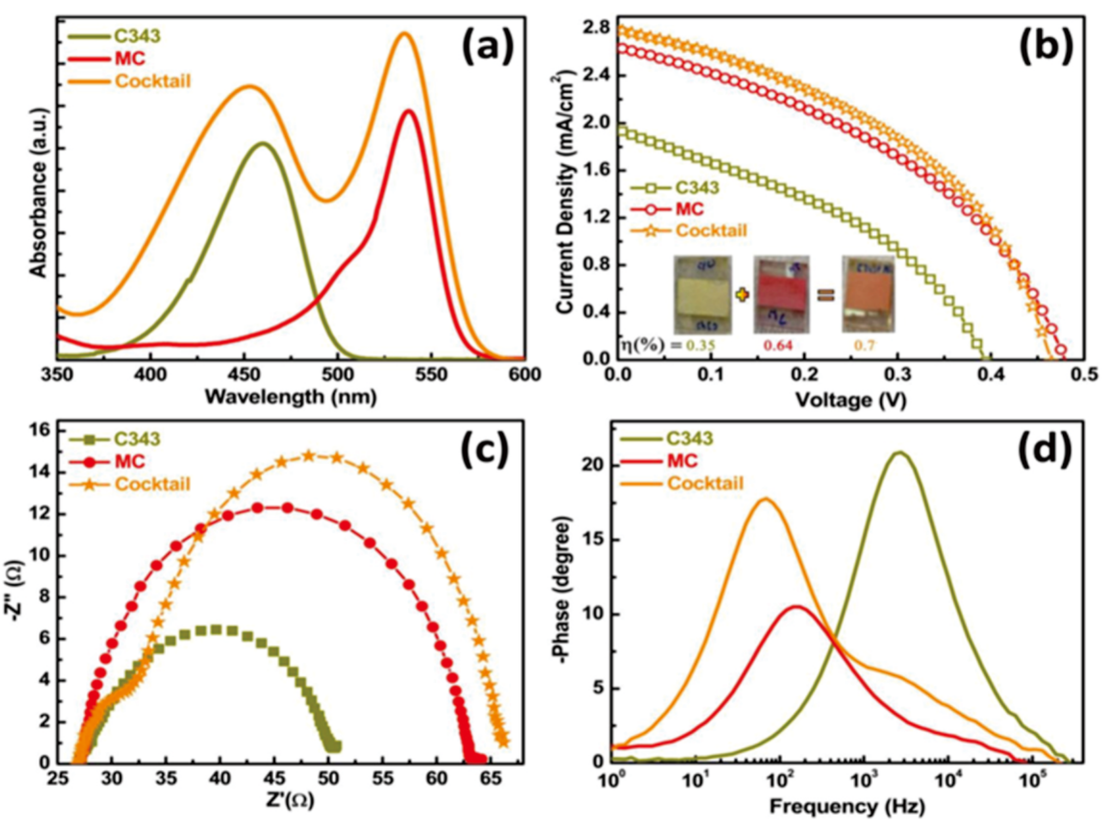

Fig. 3 **(a)** Optical absorption spectra of C343, MC and cocktail dye, **(b)** J–V characteristics, **(c)** Nyquist plot and **(d)** Bode plots of DSSCs based on C343, MC and cocktail dye sensitized Nb_2O_5 photoanode.

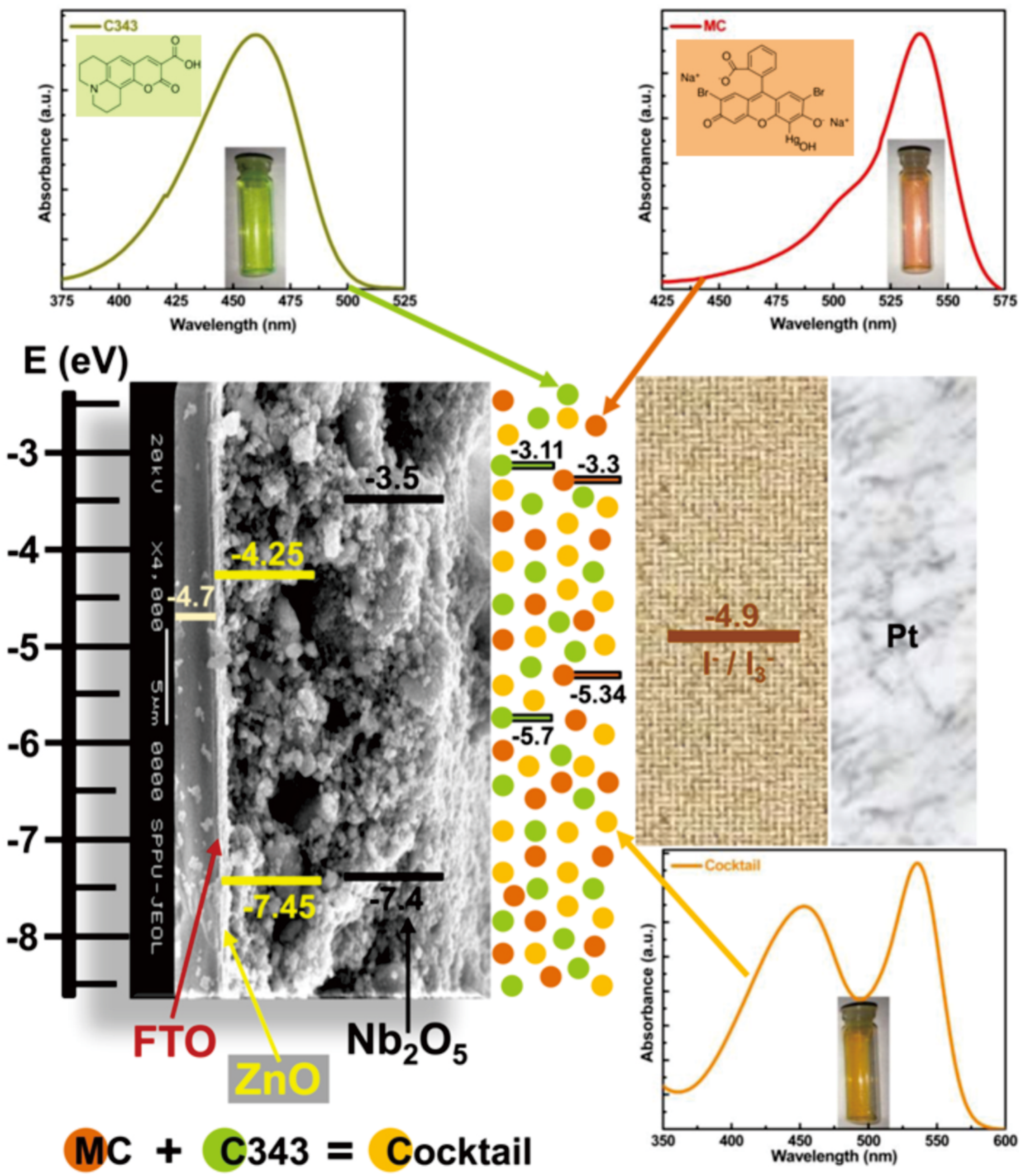

Fig. 4 Schematic device structure with energy band diagram for FTO/ZnO/Nb_2O_5/Dye/Electrolyte/Pt. Energy levels were taken from the references.[7, 42-45]

Table 2 Photovoltaic and electrochemical performance of C343, MC, cocktail dye sensitized ZnO/Nb_2O_5 photoanode based DSSCs.

Dye	Amount of dye adsorbed (x 10^{-8} M/cm^2)		J_{sc} (mA/cm^2)	V_{oc} (V)	FF (%)	R_s (Ω)	R_{ct} (Ω)	τ_e (ms)	η (%)
	C343	MC							
C343	1.13	-	1.52	0.42	44.6	27.0	23.4	0.06	0.35
MC	-	2.12	2.64	0.47	40.7	26.9	36.4	1.1	0.64
C343+MC	0.95	1.50	2.78	0.46	43.4	26.8	39.3	2.3	0.70

cells sensitized with MC and C343 dye. Table 2 summarizes the values of series resistance (R_s), R_{ct} and τ_e for all the three devices. Schematic device structure with energy band diagram for FTO/ZnO/Nb_2O_5/Dye/Electrolyte/Pt is shown in Fig. 4. When the photons get absorbed by the dye (C343/MC/cocktail dye), electrons in HOMO level get transferred to excited state, i.e. LUMO level. The CB position of Nb_2O_5 (-3.5 eV)[7] lies below LUMO level C343/MC dye (-3.11/-3.3 eV)[43-44] so that electron injection can take place easily. The CB position of Nb_2O_5 (-3.5 eV) lies above the CB position of ZnO (-4.25 eV)[45] in ZnO/Nb_2O_5 based DSSCs. ZnO used as compact layer to avoid the direct access of electrolyte to the FTO surface moreover, the ZnO compact layer with its conduction band edge being positioned above that of FTO (-4.7 eV)[46] and below that of Nb_2O_5 has favourable band position for electron transfer in Nb_2O_5 based DSSCs.

4. Conclusions

A range of low cost organic dyes having different optical absorption were adsorbed on Nb_2O_5 based photoanode with the aim to develop attractive, low cost and colorful solar cells. We have clearly demonstrated the cocktail dye (C343+MC) sensitization approach by using an equimolar mixture of inexpensive dyes. The efficiency improvement observed for the cocktail dye sensitized device is due to the enhancement in overall dye loading over Nb_2O_5 and also the absorption coverage of dye in solar spectrum. From EIS analysis it is concluded that the electron recombination resistance increase for cocktail dye based device as compared with that of C343 and MC dye based device. Hence increase in lifetime of electrons for cocktail dye sensitized Nb_2O_5 based DSSCs was observe as compared with that of C343 and MC dye based device. Mixture of two colored dyes lead to another color and enhanced the overall efficiency DSSCs. The maximum efficiency of 0.70% was achieved for Nb_2O_5 based DSSCs sensitized with cocktail dye.

Acknowledgements

Authors acknowledge Department of Science & Technology government of India for financial support vide Sanction order DST/TMD/SERI/S173(G), NIB is thankful to CSIR, New Delhi for SRF [09/137(0579)/2018-EMR-I]. PKB is thankful to University Grants Commission, New Delhi, India for the award of Dr. D. S. Kothari Post Doctoral Fellowship and financial assistance (PH/16-17/0074).

References

1. F. Gao, Y. Wang, D. Shi, J. Zhang, M. Wang, X. Jing, R. Humphry-Baker, P. Wang, S. M. Zakeeruddin and M. Gratzel, *J. Am. Chem. Soc*., 2008, **130**, 10720-10728.
2. A. K. Chandiran, S. M. Zakeeruddin, R. Humphry-Baker, M. K. Nazeeruddin, M. Gratzel and F. Sauvage, *Chem. Phys. Chem*., 2017, **18**, 2724-2731.
3. P. K. Baviskar, W. Tan, J. Zhang and B. R. Sankapal, *J. Phys D. Appl. Phys.*, 2009, **42,** 125108.
4. S. A. Arote, M. B. Rajendra Prasad, V. A. Tabhane and H. M. Pathan, *Opt. Mater*., 2015, **49,** 213-217.
5. M. A. Waghmare, M. Naushad, H. M. Pathan and A. U. Ubale, *J. Solid State Electrochem*., 2017, **21**, 2719-2723.
6. H. Zhang, Y. Wang, D. Yang, Y. Li, H. Liu, P. Liu, B. J. Wood and H. Zhao, *Adv. Mater*., 2012, **24,** 1598-1603.
7. J. Z. Ou, R. A. Rani, M. Ham, M. R. Field, Y. Zhang, H. Zheng, P. Reece, S. Zhuiykov, S. Sriram, M. Bhaskaran, R. B. Kaner and K. Kalantar-zadeh, *ACS Nano*, 2012, **6**, 4045-4053.
8. P. Du, L Song, J. Xiong, Y. Yuan, L. Wang, Z. Xi, D. Jin and J. Chen, *Electrochem. Commun*., 2012, **25**, 46-49.
9. Z. Yu, E. R. Waclawik, Z. Wang, X. Gu, Y. Yuan and Z. Zheng, *J. Mater. Chem. A*, 2017, **5**, 4607-4615.
10. C. C. Raj and R. Prasanth, *J. Power Sources*, 2016, **317,** 120-132.
11. A. L. Viet, R. Jose, M. V. Reddy, B. V. R. Chowdari and S. Ramakrishna, *J. Phys. Chem. C*, 2010, **114,** 21795-800.
12. R. Abdul, A. Sabirin, J. Subbiah, J. Zhen and K. Kalantar-zadeh, *Electrochem. Commun*., 2014, **40**, 20-23.
13. R. Ghosh, M. K. Brennaman, T. Uher, M. Ok, E. T. Samulski, L. E. McNeil, T. J. Meyer and R. Lopez, *ACS Appl. Mater. Interfaces*, 2011, **3**, 3929-3935.
14. K. Sayama, H. Sugihara and H. Arakawa, *Chem. Mater*., 1998, **10**, 3825-3832.
15. X. Jin, C. Liu, J. Xu, Q. Wang and D. Chen , *RSC Adv*., 2014, **4**, 35546-35553.
16. R. S. Mane, H. M. Nguyen, T. Ganesh, N. Kim, S. B. Ambade and S. H. Han, *Electrochem. Commun*., 2009, **11**, 752-755.
17. N. I. Beedri, S. A. A. R. Sayyed, S. R. Jadkar and H. M. Pathan, *AIP Conf. Proc*., 2017, **1832,** 040022.
18. A. K. Jana and B. B. Bhowmik, *J. Photochem. Photobiol.Chem*., 1999, **122,** 53-56.
19. C. Magne and M. Urienb, *T. Pauporte RSC Adv*., 2013, **3** , 6315-6318.
20. P. K. Baviskar, D. P. Dubal, S. Majumder, A. Ennaoui and B. R. Sankapal, *J. Photochem. Photobiol.Chem*., 2016, **318**, 135-141.
21. L. Y. Lin, M. H. Yeh, C. P. Lee, J. Chang, A. Baheti, R. Vittal, K. R. J. Thomas and K. C. Ho, *J. Power Sources*, 2014, **247**, 906-914.
22. R. Y. Ogura, S. Nakane, M. Morooka, M. Orihashi, Y. Suzuki and K. Noda, *Appl. Phys. Lett*., 2009, **94**, 073308.
23. L. H. Nguyen, H. K. Mulmudi, D. Sabba, S. A. Kulkarni, S. K. Batabyal, K. Nonomura, M. Gratzel and S. G. Mhaisalkar, *Phys. Chem. Chem. Phys*., 2012, **14**, 16182-16186.
24. C. M. Lan, H. P. Wu, T. Y. Pan, C. W. Chang, W. S. Chao, C. T. Chen, C. L. Wang, C. Y. Lin and E. W. G. Diau, *Energy Environ. Sci*., 2012, **5,** 6460-6464.
25. J. H. Yum, S. R. Jang, P. Walter, T. Geiger, F. Nuesch, S. Kim, J. Ko, M. Gratzel and M. K. Nazeeruddin, *Chem. Commun.*, 2007,**10**, 4680-4682.
26. H. Lee, J. Kim, D.Y. Kim and Y. Seo, *Org. Electron*., 2018, **52,** 103-109.
27. Y. Hao, Y. Saygili, J. Cong, A. Eriksson, W. Yang, J. Zhang, E. Polanski, K. Nonomura, S.M. Zakeeruddin, M. Gratzel, A. Hagfeldt and G. Boschloo, *ACS Appl. Mater. Interfaces*, 2016, **8**, 32797-32804.
28. G. H. Rao, A. Venkateswararao, L. Giribabu, L. Han, I. Bedja, R. K. Gupta, A. Islam and S. P. Singh, *Phys. Chem. Chem. Phys*., 2016, **18**,14279-14285.
29. C. H. Lee, S. A. Kim, M. R. Jung, K. S. Ahn, Y. S. Han and J. H. Kim, *Jpn. J. Appl. Phys*., 2014, **53**, 08NC04.
30. L. Yu, K. Fan, T. Duan, X. Chen, R. Li and T. Peng, *ACS Sustainable Chem. Eng*., 2014, **2,** 718-725.
31. P. Baviskar, R. Gore, A. Ennaoui and B. Sankapal, *Mater. Lett*., 2014, **116** , 91-93.
32. Y. T. Huang, R. Cheng, P. Zhai, H. Lee, Y. H. Chang and S. P. Feng, *Electrochim. Acta*, 2017, **236,** 131-139.
33. N. I. Beedri, P. K. Baviskar, V. P. Bhalekar, C. V. Jagtap, Innamudin, A. M. Asiri, S. R. Jadkar and H. M. Pathan, *Phys Status Solidi (A)*, 2018, **215**, 1800236.
34. R. Ahmad, N. Tripathy, M. Ahn and Y. Hahn, *Sci. Rep*., 2017, **7**, 46475.
35. P. Du, L Song, J. Xiong, Y. Yuan, L. Wang, Z. Xi, D. Jin and J. Chen, *Electrochem. Commun*., 2012, **25**, 46-49.
36. R. A. Rani, A. S. Zoolfakar, J. Subbiah, J. Z. Ou and K. Kalantar-zade*h, Electrochem. Commun*., 2014, **40**, 20-23.
37. L. Chu, W. Liu, A. Yu, Z. Qin, R. Hu, H. Shu, Q. P. Luo, Y. Min, J. Yang and X. Li, *Sol. Energ*., 2017, **153**, 584-589.
38. M. P. F. Graça, A. Meireles, C. Nico and M. A. Valente, *J. Alloy. Compd*., 2013, **553**, 177-182.
39. Q. Jiang, Y. P. Yeh, N. Lu, H. W. Kuo, M. Lesslie and T. Xu, *J. Renewable Sustainable Energy*, 2016, **8,** 013701.
40. Q. Jiang, Y. Yeh, N. Lu, H. Kuo, M. Lesslie and T. Xu, *J. Renewable Sustainable Energy*, 2016, **8**, 013701.
41. H. L. Jia, M. D. Zhang, W. Yan, X. H. Ju and H. G. Zheng, *J. Mater. Chem. A*, 2016, **4**, 11782-11788.
42. S. Majumder, P. K. Baviskar and B. R. Sankapal, *Electrochim. Acta*, 2016,

222, 100-107.
43. P. Ho, S. Thogiti, Y. H. Lee and J. H. Kim, *Sci. Rep.*, 2017, **7**, 2272.
44. K. Hara, T. Horiguchi, T. Kinoshita, K. Sayama, H. Sugihara and H. Arakawa, *Sol. Energy Mater. Sol. Cells*, 2000, **64,** 115-134.
45. S. Huang, W. Luo and Z. Zou, *J. Phys. D: Appl. Phys*., 2013, **46**, 235108.
46. K. Basu, D. Benetti, H. Zhao, L. Jin, F. Vetrone, A. Vomiero and F. Rosei, *Sci. Rep*., 2016, **6,** 23312.